Wave-induced stresses and pore pressures near a mudline

Andrzej Sawicki
Ryszard Staroszczyk[*]

Institute of Hydroengineering,
Polish Academy of Sciences,
(IBW PAN),
Kościerska 7, PL–80–328 Gdańsk, Poland;

e-mail: as@ibwpan.gda.pl, rstar@ibwpan.gda.pl

[*]corresponding author

Abstract

Conventional methods for the determination of water-wave induced stresses in seabeds composed of granular soils are based on Biot-type models, in which the soil skeleton is treated as an elastic medium. Such methods predict effective stresses in the soil that are unacceptable from the physical point of view, as they permit tensile stresses to occur near the upper surface of the seabed. Therefore, in this paper the granular soil is assumed to behave as an elastic-ideally plastic material, with the Coulomb-Mohr yield criterion adopted to bound admissible stress states in the seabed. The governing equations are solved numerically by a finite difference method. The results of simulations, carried out for the case of time-harmonic water waves, illustrate the depth distributions of the excess pore pressures and the effective stresses in the seabed, and show the shapes of zones of soil in the plastic state. In particular, the effects on the seabed behaviour of such parameters as the degree of pore water saturation, the soil permeability, and the earth pressure coefficient, are illustrated.

The complete text of the paper is available at http://www.iopan.gda.pl/oceanologia/

1. Introduction

The mechanics of a seabed, particularly near a mudline, is of great importance in many fields – coastal engineering, geomorphology, sedimentology and groundwater hydrology, to mention just a few (Massel et al. 2004, 2005). One of the basic problems concerns water-seabed interactions, including the influence of water waves on the dynamics of the upper part of the seabed near a mudline. Pressure changes at the mudline caused by water waves induce corresponding changes in pore pressures and associated changes in stresses in the soil skeleton, according to the following relations for plane strain conditions:

$$\sigma_x' = \sigma_x + u, \tag{1}$$

$$\sigma_z' = \sigma_z + u, \tag{2}$$

where u is pore water pressure (positive in compression), σ_x and σ_z denote global normal stresses treated as negative in compression, and σ_x' and σ_z' denote effective normal stresses.

Equations (1) and (2) show that the magnitudes of (compressive) effective stresses in the subsoil decrease as the pore pressure increases. Our aim is to describe these stress changes, using the methods of applied mechanics. Researchers have been working on this problem for more than half a century. Developments in modelling are discussed in Sawicki & Mierczyński (2006) (see also Sumer & Fredsøe 2002). A wide range of models have been applied to describe the interactions between water waves and the seabed, starting with a rigid skeleton and incompressible water, and ending up with introducing water compressibility and elasticity of the soil skeleton, etc. For the relevant references, see Sawicki & Mierczyński (2006). At present, it seems that the model formulated by Yamamoto et al. (1978), based on the Biot (1941) equations, is used as a kind of standard. This model takes into account both the soil skeleton elasticity and the compressibility of the pore water, and assumes that the motion of the latter relative to the porous skeleton is governed by Darcy's law. The same assumptions have been adopted to develop a number of other theories, for instance, those by Madsen (1978) and Mei & Foda (1981).

However, the approach proposed by Yamamoto et al. (1978) has several shortcomings that strongly influence the distribution of effective stresses in the seabed, particularly in a practically important upper layer, e.g. near a mudline (Sawicki & Mierczyński 2005). The main shortcoming is that the effective stresses in this region are statically inadmissible, which physically means that such stress states cannot occur in real granular soils. The

condition which bounds these effective stresses follows from the well-known Coulomb-Mohr criterion:

$$f = (\sigma'_z - \sigma'_x)^2 - (\sigma'_z + \sigma'_x)^2 \sin^2 \varphi + 4(\tau_{xz})^2 = 0, \tag{3}$$

where φ is the angle of internal friction, and τ_{xz} is the shearing stress component of the effective stress tensor. In this study, a rectangular co-ordinate system is employed, in which the vertical axis z is directed downwards, and the horizontal axis x coincides with the mudline. Equation (3) should be incorporated into the system of the problem-governing equations, such as the equilibrium/motion and mass balance relations. Sawicki & Staroszczyk (2008) have shown that inclusion of the Coulomb-Mohr condition in the analysis leads to a very different distribution of wave-induced excess effective stresses in a seabed compared to that predicted by the Yamamoto et al. (1978) theory.

In this paper, attention will focus on the water-wave induced pore pressures and effective stresses that develop near a mudline. In this region, sediment transport takes place, and it is therefore important to estimate its depth, as well as the stress state in this layer. On the other hand, the results obtained may be of some importance for the interpretation of experiments performed in wave channels, such as those described by Massel et al. (2004, 2005). For this reason, the numerical results, presented later in Section 4, correspond to such experiments.

2. Formulation of the problem

The static scheme of the problem considered is shown in Figure 1. The thickness of the porous seabed is taken to be D. The seabed, consisting of a granular soil, is based on a rigid and impervious stratum. The depth of still water is denoted by h.

It is assumed that stresses in the seabed are generated by time-harmonic standing water waves. Such waves can result from the reflection of progressive waves from the vertical walls of hydro-engineering structures. The analysis of standing waves is important, as they are known to be more conducive to seabed scour than the progressive waves.

If the standing wave height is denoted by H and its length by L, the pressure which the wave exerts on the seabed at the mudline $z = 0$ is described by the relation:

$$u_0 = u_b \sin(kx) \sin(\omega t), \tag{4}$$

where $k = 2\pi/L$ is the wave number, $\omega = 2\pi/T$ is the angular frequency, t is the time, T is the wave period, and
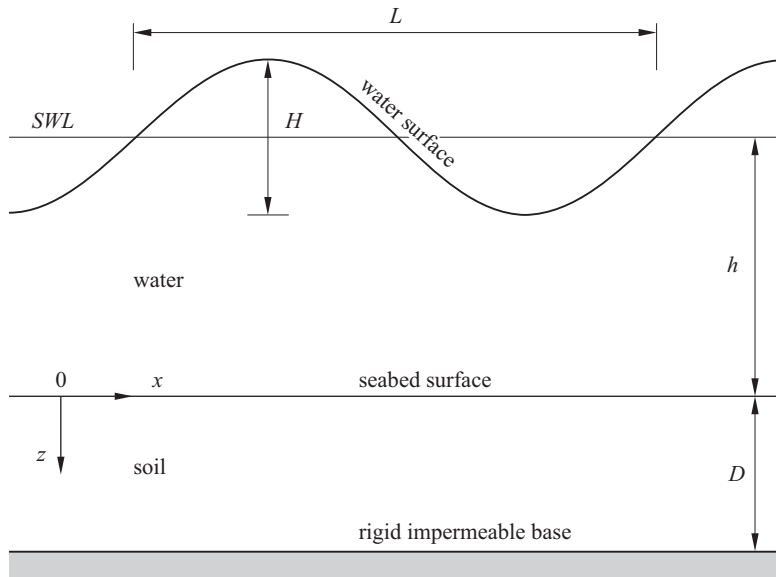
Figure 1. Water wave of height H and length L over a porous seabed of depth D

$$u_b = \frac{\gamma_w H}{2\cosh(kh)}, \tag{5}$$

where γ_w is the unit weight of water.

The water wave pressure (4) is the boundary condition for the pore pressure in the seabed. Further, the effective stresses in the soil skeleton are zero at the mudline. Thus, the boundary conditions at the upper surface of the seabed are expressed by

$$z = 0: \quad u = u_0, \quad \sigma'_z = 0, \quad \tau_{xz} = 0. \tag{6}$$

At the lower surface of the seabed, owing to the assumed impermeability and rigidity of the underlying base, the boundary conditions are defined by

$$z = D: \quad \frac{\partial u}{\partial z} = 0, \quad w_x = 0, \quad w_z = 0, \tag{7}$$

where w_x and w_z denote the respective components of the soil skeleton displacements. Because of the periodicity of the phenomenon under consideration, the analysis can be confined to a region containing only one, or a few, water wavelengths. Hence, for any x, z and t, the following periodic boundary conditions are satisfied:

$$\mathcal{A}(x, z, t) = \mathcal{A}(x \pm jL, z, t), \quad (j = 1, 2, \ldots), \tag{8}$$

with $\mathcal{A}$ representing any of the soil stress or displacement components.

Within the soil layer, $0 \leq z \leq D$, the following equilibrium equations, relating the effective stresses and the excess pore pressure, should be satisfied:

$$\frac{\partial \sigma'_x}{\partial x} + \frac{\partial \tau_{xz}}{\partial z} - \frac{\partial u}{\partial x} = 0, \tag{9}$$

$$\frac{\partial \sigma'_z}{\partial z} + \frac{\partial \tau_{xz}}{\partial x} - \frac{\partial u}{\partial z} + \gamma_{sat} = 0, \tag{10}$$

with

$$\gamma_{sat} = n\gamma_w + (1 - n)\gamma_g, \tag{11}$$

where n denotes the porosity of the soil, and γ_g is the unit weight of solid grains.

The excess effective stresses, satisfying equations (9) and (10), are imposed on the initial geostatic stress state, defined by

$$\sigma'_x = K_0 \sigma'_z, \tag{12}$$

$$\sigma'_z = -(\gamma_{sat} - \gamma_w)z, \tag{13}$$

where K_0 denotes the coefficient of earth pressure at rest.

The equilibrium relations (9) and (10) are supplemented by the storage equation that takes into account the effects of Darcy's filtration law and the mass balance of pore water (Verruijt 1969):

$$\frac{k_f}{\gamma_w} \nabla^2 u = \frac{n}{K'} \frac{\partial u}{\partial t} + \frac{\partial \varepsilon}{\partial t}, \tag{14}$$

where k_f is the filtration coefficient of the soil skeleton, K' is the apparent bulk modulus of pore water, $\varepsilon = \varepsilon_x + \varepsilon_z$ (where ε_x and ε_z are the axial strain tensor components) is the volumetric strain, and ∇^2 denotes the Laplacian operator.

The apparent bulk modulus of water depends on the degree of saturation of the soil pores by water. After Verruijt (1969), the following relation is adopted here to describe the value of K' in terms of the water saturation coefficient, denoted by S:

$$\frac{1}{K'} = \frac{S}{K} + \frac{1 - S}{p_0}, \tag{15}$$

where K is the true bulk modulus of water (that is, without any air bubbles, $S = 1$), and p_0 is the absolute pressure in the pore water. Assuming that $K = 1.9 \times 10^9$ Pa and $p_0 = 10^5$ Pa, the latter formula gives for $S = 0.99$ (1% of air content in water) the value of $K' \approx 10^7$ Pa, and for $S = 0.95$

(5% of air) the value of $K' \approx 2 \times 10^6$ Pa, showing a significant decrease in the water bulk modulus with even a relatively small amount of gas entrapped in the pore water.

The system of equations (9), (10) and (14) defines the already classical approach by Yamamoto et al. (1978), provided that Hooke's law is additionally assumed, implying that the effective stresses cause only elastic changes in the soil strains. In the present paper a more realistic model of the soil skeleton behaviour is assumed, as mentioned in the Introduction. The model is based on the simplest approach of the elastic-ideal plastic behaviour of the soil skeleton. This means that the total strain tensor, $\boldsymbol{\varepsilon}$, is decomposed into elastic, $\boldsymbol{\varepsilon}^{el}$, and plastic, $\boldsymbol{\varepsilon}^{pl}$, parts:

$$\boldsymbol{\varepsilon} = \boldsymbol{\varepsilon}^{el} + \boldsymbol{\varepsilon}^{pl}. \tag{16}$$

It is assumed that the elastic part of the strain is described by Hooke's law. However, in comparison with the classical formulation, an important modification is introduced, in which the skeleton shear modulus, G, depends on the mean effective stress, p'. That is,

$$G = G(p'), \tag{17}$$

where, in the initial geostatic stress state,

$$p' = -\frac{1}{3}\left(1 + 2K_0\right)\sigma'_z. \tag{18}$$

A general form of relation (17) follows from experimental observations that the shear modulus of granular soil strongly depends on the mean effective stress. For example, Sawicki & Mierczyński (2005) have proposed the following specific form of this relation:

$$G = G_0 \left(1 + 4\,\frac{p'}{p^*}\right), \tag{19}$$

where G_0 is the residual value of the shear modulus, and $p^* = 10^5$ Pa is a stress unit. Other specific forms of (17) are also possible, depending on experimental data. In this paper, for simplicity, it is assumed that $G = \text{const}$, as was done, for instance, by Massel et al. (2005).

The plastic components of the strain tensor are supposed to be governed by the associated flow rule expressed by

$$\dot{\boldsymbol{\varepsilon}}^{pl} = \dot{\lambda}\,\frac{\partial f}{\partial \boldsymbol{\sigma}'}, \tag{20}$$

where $\dot{\boldsymbol{\varepsilon}}^{pl}$ is an increment of the plastic strain tensor, and $\dot{\lambda}$ is a scalar multiplier.

Combination of Hooke's law and the associated flow rule leads to the following relations for the total strain increments:

$$\dot{\varepsilon}_x = \frac{1}{2G}\left[(1-\nu)\dot{\sigma}'_x - \nu\dot{\sigma}'_z\right] + 2\dot{\lambda}\left[\sigma'_x\cos^2\varphi - \sigma'_z(1+\sin^2\varphi)\right], \qquad (21)$$

$$\dot{\varepsilon}_z = \frac{1}{2G}\left[-\nu\dot{\sigma}'_x + (1-\nu)\dot{\sigma}'_z\right] + 2\dot{\lambda}\left[-\sigma'_x(1+\sin^2\varphi) + \sigma'_z\cos^2\varphi\right], \quad (22)$$

$$\dot{\varepsilon}_{xz} = \frac{1}{2G}\dot{\tau}_{xz} + 8\dot{\lambda}\tau_{xz}, \tag{23}$$

where the superimposed dots denote increments of respective strain and stress quantities, and ν denotes the Poisson ratio of the soil skeleton.

The above equations should be supplemented by a condition, holding during plastic deformation, that subsequent effective stress increments are tangential to the yield surface $f = 0$. In a general form, this condition is expressed by

$$\frac{\partial f}{\partial \boldsymbol{\sigma}'}\,\mathrm{d}\boldsymbol{\sigma}' = 0, \tag{24}$$

which, for the specific situation considered, when the Coulomb-Mohr condition defined by equation (3) is applied, gives

$$\left[\sigma'_x\cos^2\varphi - \sigma'_z(1+\sin^2\varphi)\right]\dot{\sigma}'_x +$$
$$+ \left[-\sigma'_x(1+\sin^2\varphi) + \sigma'_z\cos^2\varphi\right]\dot{\sigma}'_z + 4\tau_{xz}\dot{\tau}_{xz} = 0. \tag{25}$$

The plane-strain problem considered is described by the system of seven equations: (9), (10), (14), (21)–(23), and either (3) or (25), but involves eight unknown functions: σ'_x, σ'_z, τ_{xz}, u, ε_x, ε_z, ε_{xz} and $\dot{\lambda}$. In order to solve the equations, the number of unknown variables is reduced by a standard method, that is, by introducing the plane displacement components, w_x and w_z, in terms of which the strains, treated here as infinitesimally small, are expressed by

$$\varepsilon_x = \frac{\partial w_x}{\partial x}, \quad \varepsilon_z = \frac{\partial w_z}{\partial z}, \quad \varepsilon_{xz} = \frac{1}{2}\left(\frac{\partial w_x}{\partial z} + \frac{\partial w_z}{\partial x}\right). \tag{26}$$

In this way, the number of unknowns is reduced by one. Further reduction is achieved by using the constitutive relations (21)–(23) to express the effective stresses in terms of the skeleton displacements as well. After inserting the resulting relations for the stresses into equations (9) and (10), and using (26) to express the volumetric strain $\varepsilon = \varepsilon_x + \varepsilon_z$ in (14), the problem is transformed to the solution of a system of four equations. These

are: two equilibrium balances, the storage equation, and the plastic yield condition, and involve four independent variables: two displacements w_x and w_z, the excess pore water pressure u, and the function $\dot{\lambda}$. The respective boundary conditions are defined by equations (4)–(8). In the case of a purely elastic response of the soil, that is when plastic yield does not occur, only the equilibrium and the storage equations are solved, with $\dot{\lambda} = 0$ set in the former.

3. Numerical method

The governing equations presented in the previous section have a clear physical interpretation that simplifies the understanding of the processes modelled. However, the structure of the system of four equations to be solved is complex: the two equilibrium and the storage equations are partial differential equations, which are second-order in spatial and first-order in temporal variables, and the fourth equation, that expressing the plastic yield condition, is a non-linear algebraic relation. For this reason, special numerical techniques need to be applied to ensure the convergence and stability of the computational algorithm.

The three differential equations, for w_x, w_z and u, have been solved numerically by using a finite difference method to discretize the problem in space. The ensuing set of semi-discrete equations is solved in the time domain by applying a single-step implicit scheme, the so-called weighted-average method (also known as the θ-method) – see, for instance, Zienkiewicz & Taylor (2000a). In the case of purely elastic behaviour, while the resulting effective stress states lie inside the yield surface (that is, when $f < 0$ in equation (3)), the solution procedure does not cause any serious numerical difficulties. However, when a plastic process is active within the seabed, then, apart from the above three differential equations, also the fourth, the yield equation $f = 0$, must be solved for each discrete point at which plastic flow occurs. This poses additional numerical problems that must be treated with care.

Several methods are available for numerical modelling of the elastic-plastic behaviour of materials. In this work, the most common approach – the method of increments – was used. At each time step, that is within an increment of the wave-induced loading, an iterative procedure was applied to determine the soil stresses corresponding to the current displacement increments (and hence the current total strains) obtained from the system of equilibrium and storage equations. For this purpose, a method known as the return map algorithm was employed (Zienkiewicz & Taylor 2000b). In this fully implicit method, the three constitutive relations (21)–(23), combined with the yield condition (3), were solved to calculate the stress

increments; this ensured that the current total effective stress state was exactly on the yield surface (alternatively, equation (25) could have been used instead of (3), but in that case the convergence to the exact solution would have been much slower). The four, strongly non-linear, equations for the three stress increments, $\dot{\sigma}'_x$, $\dot{\sigma}'_z$ and $\dot{\tau}_{xz}$, and the coefficient $\dot{\lambda}$, were solved for each discrete node separately using the Newton-Raphson method.

The effective stresses calculated by the above procedure did not, in general, satisfy the initial equilibrium equations for a current load increment, since the occurrence of plastic yield led to the re-distribution of the stresses in the soil skeleton. Therefore, a series of iterations had to be executed recurrently, with repeatedly updated plastic strains to calculate new displacements, then total strains, and finally new stresses, until all the quantities involved became balanced for a given load increment. These iterations were carried out by using a direct (or Picard) iteration method that turned out to be more efficient for this task than the usual Newton-Raphson method.

The finite difference computations were carried out for the domain of the length L (that is, equal to the water wavelength), and of the height D, equal to the seabed thickness. On this domain, a uniform rectangular grid with 51 discrete nodes along the horizontal, and 201 nodes along the vertical, was imposed. The time integration was conducted with a time step length $\Delta t = T/100$. The stresses during plastic loading were balanced with a relative error of 10^{-8}, the equilibrium and the storage equations were solved with a relative error of 10^{-5} between two successive iterations. For numerical reasons, to maintain stability of the algorithm, the height of the water wave was increased in a smooth manner from zero to its prescribed value H over the time interval of three wave periods. The results presented in the next section are those calculated for the times of at least five wave periods, that is, for $t \geq 5T$.

Before employing our discrete model in simulations of the elastic-plastic response of the seabed, it was validated by comparing the model predictions for the simpler case of the purely elastic response with the results presented by Sawicki and Mierczyński (2005). The latter were obtained, like the results of Yamamoto et al. (1978), by applying the Biot equations. Comparison of the present model predictions with those given by Sawicki & Mierczyński (2005), obtained for the input data adopted from Hsu & Jeng (1994), showed good agreement, with the maximum relative differences between the respective effective stress tensor components and the pore pressures not exceeding 2%. The correctness of the proposed numerical model was thus confirmed.

4. Simulations of seabed behaviour

Simulations of seabed behaviour under the action of water waves have been performed for the data roughly corresponding to the laboratory investigations carried out by Massel et al. (2004, 2005). Hence, the following parameters reported in these two papers were used in numerical calculations: the mean water depth $h = 2$ m, the subsoil thickness $D = 2$ m, the water wave period $T = 5$ s, corresponding to a wave length of $L = 20.95$ m, the soil porosity $n = 0.26$, the soil shear modulus $G = 3.8 \times 10^7$ Pa, and the soil filtration coefficient $k_f = 2.9 \times 10^{-4}$ m s^{-1}. Moreover, a few parameters corresponding to typical sand properties were assumed: the skeleton Poisson ratio $\nu = 0.3$, the unit weight of grains $\gamma_g = 2.65 \times 10^4$ N m^{-3}, the internal friction angle $\varphi = 30°$, and the coefficient of earth pressure at rest $K_0 = 0.5$. The simulations were carried out for water wave heights H ranging from 0.2 to 0.8 m.

Figure 2 shows the distribution of pore water pressure amplitudes with the dimensionless depth z/D for different values of the pore water saturation degree S. The pressure amplitudes are plotted in normalized forms u/u_b, where u_b, defined by (5), is the amplitude of the water-wave induced pressure at the mudline. Note that the presence of air in pore water considerably
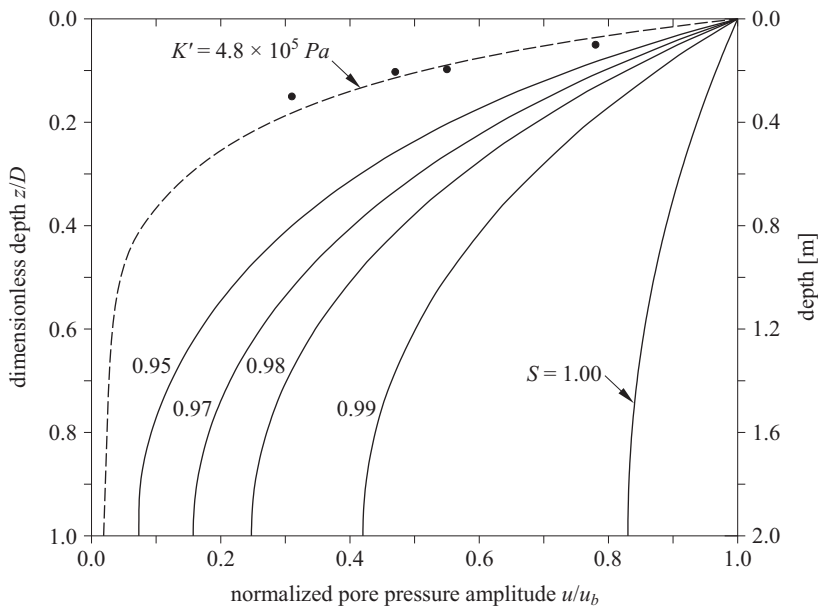

Figure 2. Depth profiles of normalized wave-induced pore water pressure amplitudes, u/u_b, as a function of the saturation coefficient S. Solid dots show experimental results measured by Massel et al. (2005)

influences the rate at which pore pressure attenuates within the seabed. While in the case of $S = 1$ (no air in water) the maximum pressure at the bottom of the seabed layer ($z = D$) is equal to about 83% of that at the mudline ($z = 0$), the presence of, say, 2% of air in pore water ($S = 0.98$) leads to a reduction in the maximum pressures at $z = D$ to a value of about 25% of that at the mudline. The solid circles in the figure present the experimental results obtained by Massel et al. (2005). These were measured for a water wave of height $H = 0.3$ m and the effective bulk modulus of water $K' = 4.8 \times 10^5$ Pa. This particular value of K' was inferred by comparing the experimental data with the predictions of the theory proposed in the previously-cited paper. In view of relation (15), the latter magnitude of K' corresponds to a rather high air content in the pore water, equal to about 20%, that is, to the saturation coefficient $S \sim 0.8$. The dashed line in Figure 2 displays the pressure amplitude depth profile calculated by our numerical model for $K' = 4.8 \times 10^5$ Pa. This profile is quite similar to that obtained by Massel et al. (2005) by their analytical solution (see Figure 2 on p. 308 in that paper).

Figures 3 to 6 (see p. 550, 551, 552) illustrate the influence of various soil parameters and the water wave height H on the maximum extent of zones in which the soil is in the plastic state, that is, where the Coulomb-Mohr failure condition (3) has been reached. Accordingly, the depth positions of the interfaces separating the part of the seabed at plastic flow (occurring between the respective lines and the mudline) and the part responding elastically are displayed. The left and right halves of the plots correspond to the regions under the wave crests and troughs, respectively.

Figure 3 presents the results obtained for a water wave of height 0.5 m, for a set of various values of the pore water saturation degree S. The plots in the figure show that the presence of air in the pore water reduces the depth of soil plastification (see Figure 2). But even for $S = 0.9$ (10% air content), the plastic zone reaches a depth of some 10 cm. This result practically means that small amplitude waves in the coastal zone may lead to the plastic state of the upper layer of the seabed. In such a state, the saturated soil is very susceptible to additional excitations like, for example, those caused by water currents. The results obtained may therefore be of some importance to researchers modelling sediment transport phenomena.

It is generally accepted that there is usually a few percent of gas entrapped in pores of natural sandy seabeds — reliable empirical measurements of the gas content in water-saturated soils are still scarce. The subsequent plots, presented in Figures 4 to 7 (see p. 550, 551, 552), illustrate the results of numerical simulations conducted for soil containing 2% of air in
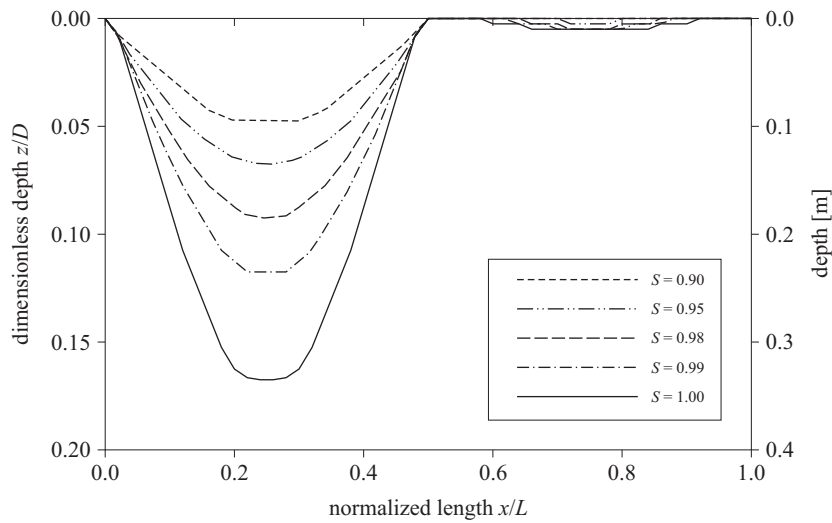
Figure 3. Maximum extent of the soil at plastic yield for different values of the pore water saturation degree S ($H = 0.5$ m, $K_0 = 0.5$)
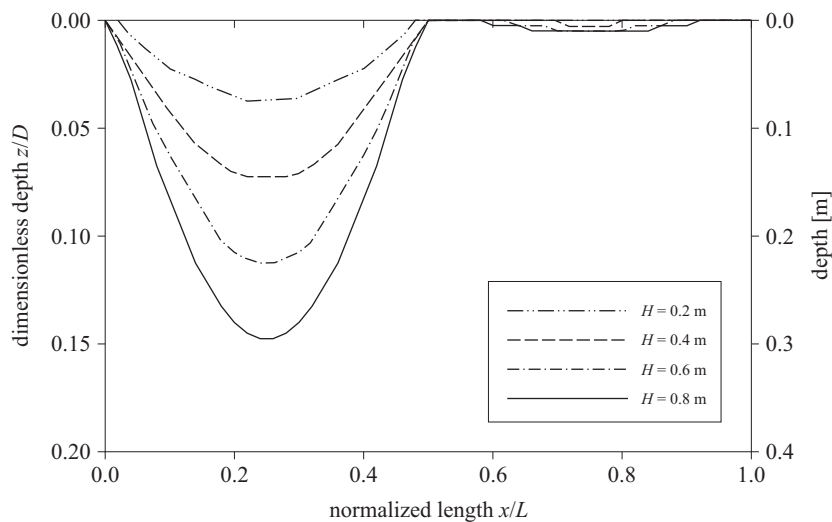

Figure 4. Maximum extent of the soil at plastic yield for different values of the water wave height H ($S = 0.98$, $K_0 = 0.5$)

its pore water, that is, for a saturation coefficient $S = 0.98$. Figure 4 confirms the intuition that the height of a water wave affects the depth of the plastic zone in the soil layer: higher waves penetrate the seabed more deeply. It can also be observed that the maximum extent of the plastic region under the wave crest is approximately proportional to the wave height: for a wave

of height 80 cm the depth of the plastic zone is about 30 cm, while for one of height 20 cm it is about 7 cm.

Figure 5 shows the influence of the coefficient of the earth pressure at rest, K_0, on the size of the plastic zone in the seabed; it will be recalled that this coefficient is defined in equation (12). The practical determination of K_0 is a difficult problem in geotechnical engineering. Small values of K_0 correspond to freshly deposited sands, higher values to compacted subsoils. It is seen in the figure that even for a high value of K_0 there is a small region in the seabed that is in the plastic state.
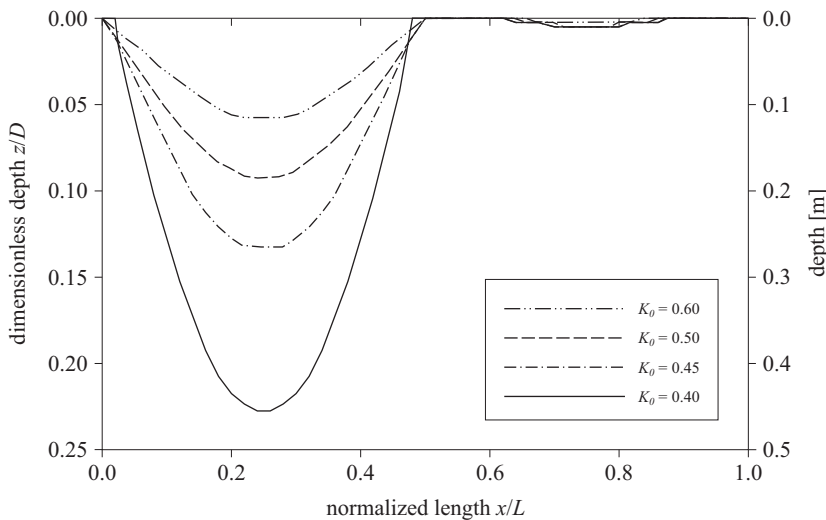

Figure 5. Maximum extent of the soil at plastic yield for different values of the earth pressure coefficient K_0 ($H = 0.5$ m, $S = 0.98$)

Figure 6 illustrates the effect of soil permeability on soil behaviour, showing the shapes of the plastic zones in the seabed for different values of the filtration coefficient k_f. It is seen that for less permeable soils the plastic regions are shallower. This is due to the fact that in less permeable soils the depth attenuation of pore pressures applied at the upper surface of the seabed layer is stronger; hence, the weakening effect of the excess pore pressures on the effective stresses (see equations (1) and (2)) is limited to the regions of smaller depth.

Finally, Figure 7 presents the depth profiles of the wave-induced excess (that is, above the geostatic state) effective stresses in the seabed for a wave height $H = 0.5$ m and a pore water saturation coefficient $S = 0.98$. Shown are the maximum magnitudes of the σ'_x and σ'_z components of the stress tensor under the wave crest (Figure 7a) and the wave trough (Figure 7b). The stresses are normalized in the same way as the pore water pressures
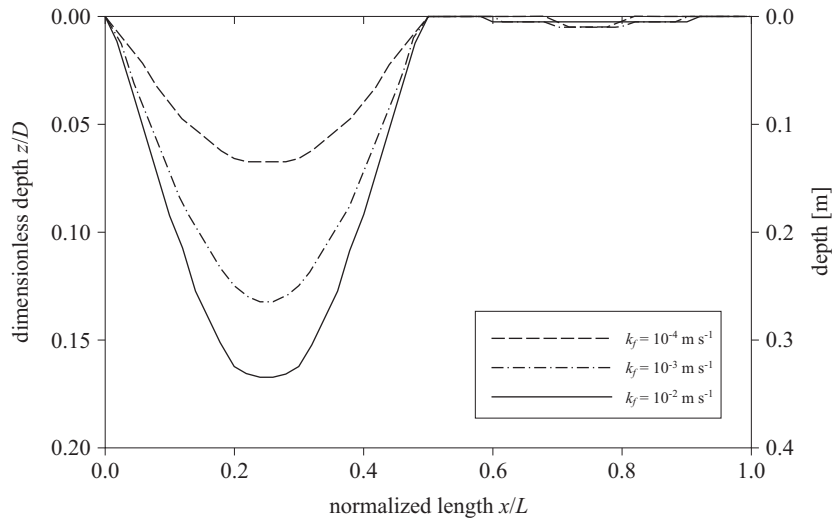
Figure 6. Maximum extent of the soil at plastic yield for different values of the soil filtration coefficient k_f ($H = 0.5$ m, $S = 0.98$, $K_0 = 0.5$)
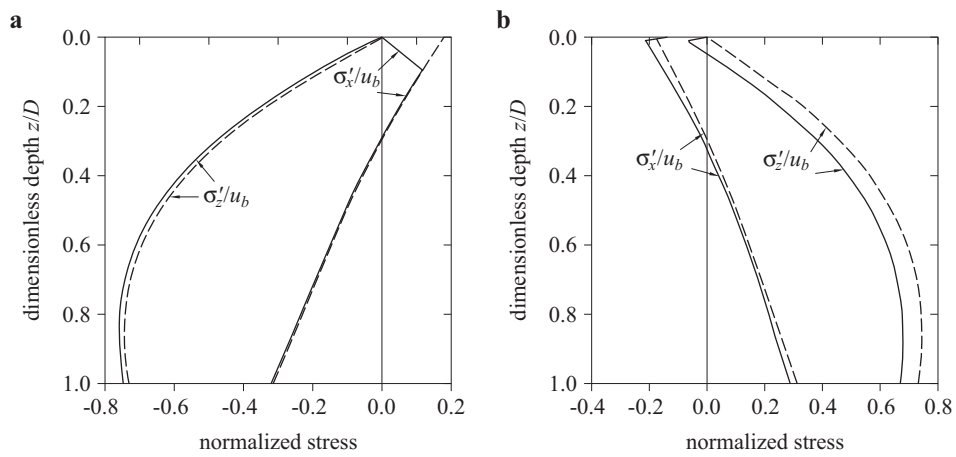

Figure 7. Depth profiles of wave-induced effective stresses σ'_x and σ'_z: (a) under the wave crest, (b) under the wave trough; (———) elastic-plastic behaviour, (– – –) purely elastic behaviour ($H = 0.5$ m, $S = 0.98$)

in Figure 2, that is, by using the seabed top surface pressure amplitude u_b, defined by (5), as a unit. The results obtained on the assumption of the elastic-plastic soil behaviour (solid lines) are compared with those for the purely elastic soil response (dashed lines). It can be seen that the elastic-plastic reaction of the seabed to the water wave loading, compared to this reaction in the elastic case, is distinct under the wave crest and the

trough. More pronounced differences occur in the subsoil under the crest. In this region, the assumption of a purely elastic response of the soil skeleton leads to tensile stresses σ'_x appearing in the upper part of the seabed (the dashed line). Such tensile stresses cannot develop when the plastic effects are permitted. Hence, a re-distribution of the stress states, so that the Coulomb-Mohr condition is fulfilled, takes place within the seabed. As a result, the σ'_x stress becomes zero at the mudline, and varies roughly linearly between $z = 0$ and the depth of the plastic zone which, in this particular case, extends to $z \approx 20$ cm, i.e., $z/D \approx 0.1$. Further below, that is under the plastic zone, the response of the seabed is purely elastic; therefore the σ'_x stress distributions for both types of soil behaviour practically coincide. As regards the σ'_z distributions under the wave crest, the differences between the elastic and elastic-plastic responses are practically negligible, which can be attributed to the fact that these stresses are compressive throughout the seabed layer; therefore, no re-distribution of stress states takes place. A qualitatively very similar elastic-plastic behaviour of the seabed near the mudline, with a significant redistribution of the σ'_x stress and a little change in the σ'_z stress compared to the purely elastic response, has been predicted by Dunn et al. (2006).

In the region under the wave trough, the elastic and elastic-plastic responses of the seabed are similar, with some shifts in the σ'_x and σ'_z magnitudes observed between the two types of soil behaviour. The re-distribution of stress states due to the plastic effects is confined to a much smaller layer just under the mudline — the thickness of the plastic zone under the trough of the wave of height 50 cm is equal to about 1.5 cm.

As regards the pore pressure distributions for the elastic and elastic-plastic responses of the water-saturated subsoil, the results of the simulations have shown, for the input conditions applied, very small differences (not exceeding 2%) along the whole depth profile, between the two cases of the seabed behaviour. This indicates the rather small influence of the plastic effects occurring near the mudline on the pore pressure distribution within the seabed layer. In the light of the above remarks on the effective stress distributions, it appears that the plasticity of the skeleton practically affects only the horizontal normal component of the stress, preventing the latter from becoming tensile near the mudline.

It is worth pointing out that, in spite of the excess effective stresses σ'_x and σ'_z being tensile in some regions within the seabed, even when the elastic-plastic behaviour is considered, the Coulomb-Mohr condition is not violated there, as these stresses are imposed on the geostatic (compressive) stress field defined by equations (12) and (13). Thus, the resulting total effective stresses in the subsoil remain compressive all the time.

5. Conclusions

The problem of water-wave induced pore pressures in the seabed has attracted the attention of researchers for more than half a century. Most of the theoretical models proposed so far are based on rather simple assumptions, which leads to unrealistic results; they include the approach of Yamamoto et al. (1978), which appears to have become a standard in marine engineering. The major shortcoming of this approach concerns the effective stresses in the seabed skeleton. Classical approaches, concentrating mainly on pore pressures, give rise to solutions which violate certain basic physical principles; for instance, the effective stress states, associated with such pore pressure distributions, cannot occur in granular media.

In order to rectify this serious shortcoming, the classical elasto-plastic model for the soil skeleton behaviour has been incorporated in the theoretical analysis instead of the purely elastic one. The results obtained by applying such an approach differ from the classical ones, particularly in the region close to the mudline. It has been shown that in this region the soil skeleton is in the plastic state. This means that various hydrodynamic forces exerted on the seabed, such as those due to water waves or currents, may cause extensive deformations of the upper layer of the seabed. These deformations may be correlated with sediment transport, so our paper suggests some possible directions for further research.

The investigation presented in this paper is limited to the case of standing water waves, since such waves, with fixed locations of the wave crests/troughs, can cause more severe scouring of the bed than comparable progressive waves. The analysis of the latter waves, in the context of the elastic-plastic behaviour of the seabed, is much more complex (the time-harmonic behaviour of the waves does not entail a time-harmonic response of the underlying subsoil). Preliminary results obtained by applying the present model have shown that, at a given time, the zones of the soil in the plastic state are smaller than those created by standing waves of the same amplitude. However, in the case of progressive waves, the zones of the soil in the plastic state move, so that the whole near-mudline layer of the seabed is subject to plastification, but each point at a different time. In order to fully describe this complex phenomenon, separate research will be required.

References

Biot M. A., 1941, *General theory of three-dimensional consolidation*, J. Appl. Phys., 12 (2), 155–164.

Dunn S. L., Vun P. L., Chan A. H. C., Damgaard J. S., 2006, *Numerical modelling of wave-induced liquefaction around pipelines*, J. Waterw. Port C.–ASCE, 132 (4), 276–288.

Hsu J. R. C., Jeng D. S., 1994, *Wave-induced soil response in an unsaturated anisotropic seabed of finite thickness*, Int. J. Numer. Anal. Met., 18 (11), 785–807.

Madsen O. S., 1978, *Wave-induced pore pressure and effective stresses in a porous bed*, Géotechnique, 28 (4), 377–393.

Massel S. R., Przyborska A., Przyborski M., 2004, *Attenuation of wave-induced groundwater pressure in shallow water. Part 1*, Oceanologia, 46 (3), 383–404.

Massel S. R., Przyborska A., Przyborski M., 2005, *Attenuation of wave-induced groundwater pressure in shallow water. Part 2. Theory*, Oceanologia, 47 (3), 291–323.

Mei C. C., Foda M. A., 1981, *Wave-induced responses in a fluid-filled poro-elastic solid with a free surface – a boundary layer theory*, Geophys. J. Roy. Astr. S., 66 (3), 597–631.

Sawicki A., Mierczyński J., 2006, *Developments in modeling liquefaction of granular soils, caused by cyclic loads*, Appl. Mech. Rev., 59 (2), 91–106.

Sawicki A., Mierczyński J., 2005, *Wave-induced stresses and liquefaction in seabed according to the Biot-type approach*, Arch. Hydro-Eng. Environ. Mech., 52 (2), 131–145.

Sawicki A., Staroszczyk R., 2008, *Stresses in a seabed due to water wave action*, [in:] *Geotechnics in maritime engineering*, Proc. 11th Baltic Sea Geotechnical Conf., Gdańsk, 743–748.

Sumer B. M., Fredsøe J., 2002, *The mechanics of scour in the marine environment*, Adv. Ser. Ocean Eng. 17, World Sci., New Jersey, 552 pp.

Verruijt A., 1969, *Elastic storage of aquifers*, [in:] *Flow through porous media*, R. J. M. De Wiest (ed.), Acad. Press, New York, 331–376.

Yamamoto T., Koning H. L., Sellmeijer H., Van Hijum E., 1978, *On the response of a poro-elastic bed to water waves*, J. Fluid Mech., 87 (1), 193–206.

Zienkiewicz O. C., Taylor R. L., 2000a, *The finite element method*, Vol. 1, *The basis*, 5th edn., Butterworth-Heinemann, Oxford, 736 pp.

Zienkiewicz O. C., Taylor R. L., 2000b, *The finite element method*, Vol. 2, *Solid mechanics*, 5th edn., Butterworth-Heinemann, Oxford, 480 pp.